

OPEN

# S1P<sub>2</sub> contributes to microglial activation and M1 polarization following cerebral ischemia through ERK1/2 and JNK

Arjun Sapkota, Bhakta Prasad Gaire, Min-Gu Kang & Ji Woong Choi

Sphingosine 1-phosphate (S1P) signaling has emerged as a drug target in cerebral ischemia. Among S1P receptors, S1P<sub>2</sub> was recently identified to mediate ischemic brain injury. But, pathogenic mechanisms are not fully identified, particularly in view of microglial activation, a core pathogenesis in cerebral ischemia. Here, we addressed whether microglial activation is the pathogenesis of S1P<sub>2</sub>-mediated brain injury in mice challenged with transient middle cerebral artery occlusion (tMCAO). To suppress S1P<sub>2</sub> activity, its specific antagonist, JTE013 was given orally to mice immediately after reperfusion. JTE013 administration reduced the number of activated microglia and reversed their morphology from amoeboid to ramified microglia in post-ischemic brain after tMCAO challenge, along with attenuated microglial proliferation. Moreover, JTE013 administration attenuated M1 polarization in post-ischemic brain. This S1P<sub>2</sub>-directed M1 polarization appeared to occur in activated microglia, which was evidenced upon JTE013 exposure *in vivo* as suppressed M1-relevant NF- $\kappa$ B activation in activated microglia of post-ischemic brain. Moreover, JTE013 exposure or S1P<sub>2</sub> knockdown reduced expression levels of M1 markers *in vitro* in lipopolysaccharide-driven M1 microglia. Additionally, suppressing S1P<sub>2</sub> activity attenuated activation of M1-relevant ERK1/2 and JNK in post-ischemic brain or lipopolysaccharide-driven M1 microglia. Overall, our study demonstrated that S1P<sub>2</sub> regulated microglial activation and M1 polarization in post-ischemic brain.

Microglia primarily regulate immune responses in the central nervous system (CNS)<sup>1</sup>. They react to brain injury and become activated to play either beneficial or detrimental roles in injured brain<sup>2</sup>. In the latter case, activated microglia are shaped as amoeboid cells<sup>3</sup> and their phenotypes are rapidly changed into M1-polarized cells<sup>4</sup>, contributing to detrimental immune responses by producing various pro-inflammatory cytokines<sup>5</sup>. These pathogenic features are well characterized in injured brain of cerebral ischemia caused by an insufficient blood flow into the brain<sup>6,7</sup>. For example, microglial activation occurs in both periischemic and ischemic core regions of the brain after a transient focal cerebral ischemia and persists up to many days<sup>8</sup>. Activated microglia at the chronic phase (over 3 days after ischemic challenge) can transform their morphology from ramified to amoeboid in the ischemic core region<sup>8–10</sup> and proliferate in the marginal zone between periischemic and ischemic core regions<sup>11</sup>. In addition, activated microglia can polarize to pro-inflammatory M1 and anti-inflammatory M2 phenotypes in post-ischemic brain, contributing to brain injury and ischemic recovery, respectively<sup>12</sup>. Given that microglial activation is a core pathogenesis in post-ischemic brain, targeting microglial activation is an emerging strategy to develop therapeutics for treating cerebral ischemia. Many efforts have been made to identify regulators of microglial activation in the post-ischemic brain<sup>6</sup>.

Sphingosine 1-phosphate (S1P), an important bioactive lysophospholipid, regulates a variety of biological functions through its five specific G protein-coupled receptors (S1P<sub>1–5</sub>) that are ubiquitously expressed throughout the body<sup>13,14</sup>. In particular, receptor-mediated S1P signaling has become an emerging drug target to treat cerebral ischemia because of FTY720' efficacy in human patients<sup>15–17</sup> and animal models<sup>18–23</sup>. Up to date, two of FTY720 efficacy-relevant S1P receptors, S1P<sub>1</sub><sup>24</sup> and S1P<sub>3</sub><sup>11</sup>, and one FTY720 efficacy-irrelevant S1P receptor, S1P<sub>2</sub><sup>25</sup>, have been identified to play a role in the pathogenesis of cerebral ischemia. Of note, the pathogenesis of cerebral ischemia *via* S1P<sub>1</sub> and S1P<sub>3</sub> is closely linked to microglial activation involving morphological changes

College of Pharmacy, Gachon University, 191 Hambakmoero, Yeonsu-gu, Incheon, 21936, Republic of Korea. Correspondence and requests for materials should be addressed to J.W.C. (email: [pharmchoi@gachon.ac.kr](mailto:pharmchoi@gachon.ac.kr))

into amoeboid cells, proliferation, and production of pro-inflammatory cytokines, a feature of M1 polarization<sup>11,24</sup>. However, it remains unknown whether S1P<sub>2</sub>-directed pathogenesis is linked into microglial activation in post-ischemic brain. It is known that the pathogenic role of S1P<sub>2</sub> in post-ischemic brain is linked to vascular dysfunction by enhancing MMP-9 activity<sup>25</sup>. Although S1P<sub>2</sub> is not elucidated as a regulator of microglial activation in post-ischemic brain yet, it can be the regulator since its role in inflammation has been reported for peripheral tissues<sup>26–28</sup>. S1P<sub>2</sub> on endothelial cells can trigger vascular dysfunction through NF- $\kappa$ B activation that subsequently results in increased production of proinflammatory mediators<sup>28</sup>. S1P<sub>2</sub> also influences inflammatory atherosclerosis by modulating the production of proinflammatory cytokines (IL-1 $\beta$  and IL-18) and macrophages activation<sup>29</sup>. Additionally, suppressing S1P<sub>2</sub> activity can attenuate acute renal ischemic injury by downregulating inflammatory cytokines<sup>27</sup>. Therefore, it is possible that S1P<sub>2</sub> could also regulate neuroinflammatory responses in the brain after ischemic challenge by activating microglia, leading to brain ischemic injury<sup>7,30,31</sup>. In addition, microglia are the main loci for S1P<sub>2</sub> expression in the brain<sup>32</sup>, suggesting that S1P<sub>2</sub> could regulate microglial activation in post-ischemic brain. This notion could be supported by a study using another disease model, in which JTE013 attenuated microglial activation and subsequent proinflammatory responses in the brain of mouse with hepatic encephalopathy<sup>33</sup>.

In this study, we aimed to address the relationship between S1P<sub>2</sub> and microglial activation in view of pathogenesis of cerebral ischemia using transient middle cerebral artery occlusion (tMCAO) in mice. Microglial activation and their morphological changes in post-ischemic brain were analyzed through Iba1 immunohistochemical analysis at both acute (1 day after tMCAO) and chronic phases (3 days after tMCAO). Moreover, we analyzed microglial proliferation and phenotypic transition, likely M1/M2 polarization, in post-ischemic brain. To demonstrate microglia as a responsible cell type for the latter, we examined *in vivo* cell polarization-relevant microglial NF- $\kappa$ B activation in post-ischemic brain and *in vitro* expression levels of cell polarization markers in BV2 microglia cell line using an inducer of M1 polarization, lipopolysaccharide (LPS). Finally, we determined M1- and S1P<sub>2</sub>-relevant downstream effector signaling in post-ischemic brain *in vivo* as well as LPS-activated BV2 microglia *in vitro*.

## Results

**Suppressing S1P<sub>2</sub> activity attenuates microglial activation and proliferation in post-ischemic brain after tMCAO challenge.** Microglia activation is a core pathogenic feature in injured brain by ischemic challenge. Microglia become activated in both the ischemic core and periischemic regions and their morphology in the ischemic core region is converted into highly detrimental type, amoeboid microglia, especially in the chronic phase (likely at least 3 days after the ischemic challenge)<sup>8–10</sup>. S1P<sub>2</sub> is a pathogenic factor for brain damage in cerebral ischemia<sup>25</sup>. Thus, we investigated whether microglial activation might play a role in S1P<sub>2</sub>-mediated brain damage in cerebral ischemia. We first determined microglial activation in both periischemic and the ischemic core regions of post-ischemic brain at 1 and 3 days after tMCAO challenge through immunohistochemical analysis for Iba1, a well-known marker for activated microglia<sup>8,34</sup>. The tMCAO challenge caused a marked increase in the number of Iba1-immunopositive cells in both periischemic and ischemic core regions at 1 day after tMCAO (Fig. 1a,b). This robust increase was significantly attenuated when S1P<sub>2</sub> activity was suppressed by oral administration of JTE013, a specific S1P<sub>2</sub> antagonist, immediately after reperfusion (Fig. 1a,b). In the chronic phase (3 days after tMCAO), the number of Iba1-immunopositive cells was increased in both regions of the injured brain (Fig. 1c,d). Suppressing S1P<sub>2</sub> activity by JTE013 administration resulted in a region-specific reduction in the number of Iba1-immunopositive cells (Fig. 1c,d). JTE013 administration significantly reduced the number of Iba1-positive cells in the periischemic region, but not in the ischemic core region at 3 days after tMCAO (Fig. 1c,d). Interestingly, in the ischemic core region at this time point, S1P<sub>2</sub> was associated with morphological changes of Iba1-immunopositive cells from ramified to amoeboid cells, another feature of microglial activation<sup>8,9</sup>. In fact, most Iba1-immunopositive cells were shaped as amoeboid in the ischemic core region at 3 days after tMCAO (Fig. 1c,e). However, after JTE013 administration, most of Iba1-immunopositive cells were shaped as ramified in the same region (Fig. 1c,e). These results clearly demonstrate that S1P<sub>2</sub> is a critical regulator for microglial activation in cerebral ischemia. In addition, we can affirm that pharmacological suppression of S1P<sub>2</sub> activity reduced brain damage at 1 and 3 days after tMCAO as evidenced by reduced neural cell death (Supplementary Fig. 1a,c) and improved neurological functions (Supplementary Fig. 1b,d) through FJB staining and mNSS scoring. Taken together, these results indicate that S1P<sub>2</sub>-regulated microglial activation could be associated with ischemic brain injury.

Activated microglia can proliferate in the injured brain after ischemic challenge. They are generally observed in the marginal zone between periischemic and ischemic core regions. Thus, we investigated whether S1P<sub>2</sub> also affected microglial proliferation in the marginal zone of the brain after tMCAO through *in vivo* BrdU incorporation and subsequent analysis of Iba1/BrdU double immunofluorescence staining. In vehicle-treated tMCAO mice, the number of Iba1/BrdU-double immunopositive cells was greatly increased in the marginal zone of post-ischemic brain (Fig. 2). However, JTE013 administration immediately after tMCAO challenge significantly attenuated such increase by approximately 70% (Fig. 2). These data demonstrate that S1P<sub>2</sub> is also involved in microglial proliferation in post-ischemic brain.

**Suppressing S1P<sub>2</sub> activity attenuates microglial M1 polarization in post-ischemic brain after tMCAO challenge.** A phenotypical change in microglial polarization with M1/M2 is an important aspect of immune responses in diverse CNS diseases<sup>35,36</sup>. In cerebral ischemia, microglia also become rapidly polarized into pro-inflammatory M1 and anti-inflammatory M2 phenotypes<sup>30</sup>. To determine whether S1P<sub>2</sub> signaling could direct microglial M1/M2 polarization, we performed qRT-PCR analysis primarily for brain samples obtained at 1 and 3 days after tMCAO. All determined soluble markers (TNF- $\alpha$ , IL-1 $\beta$ , and IL-6) and surface markers (CD11b, CD16, CD31, and CD86) for M1 polarization were upregulated in the brain challenged by tMCAO at both 1 and

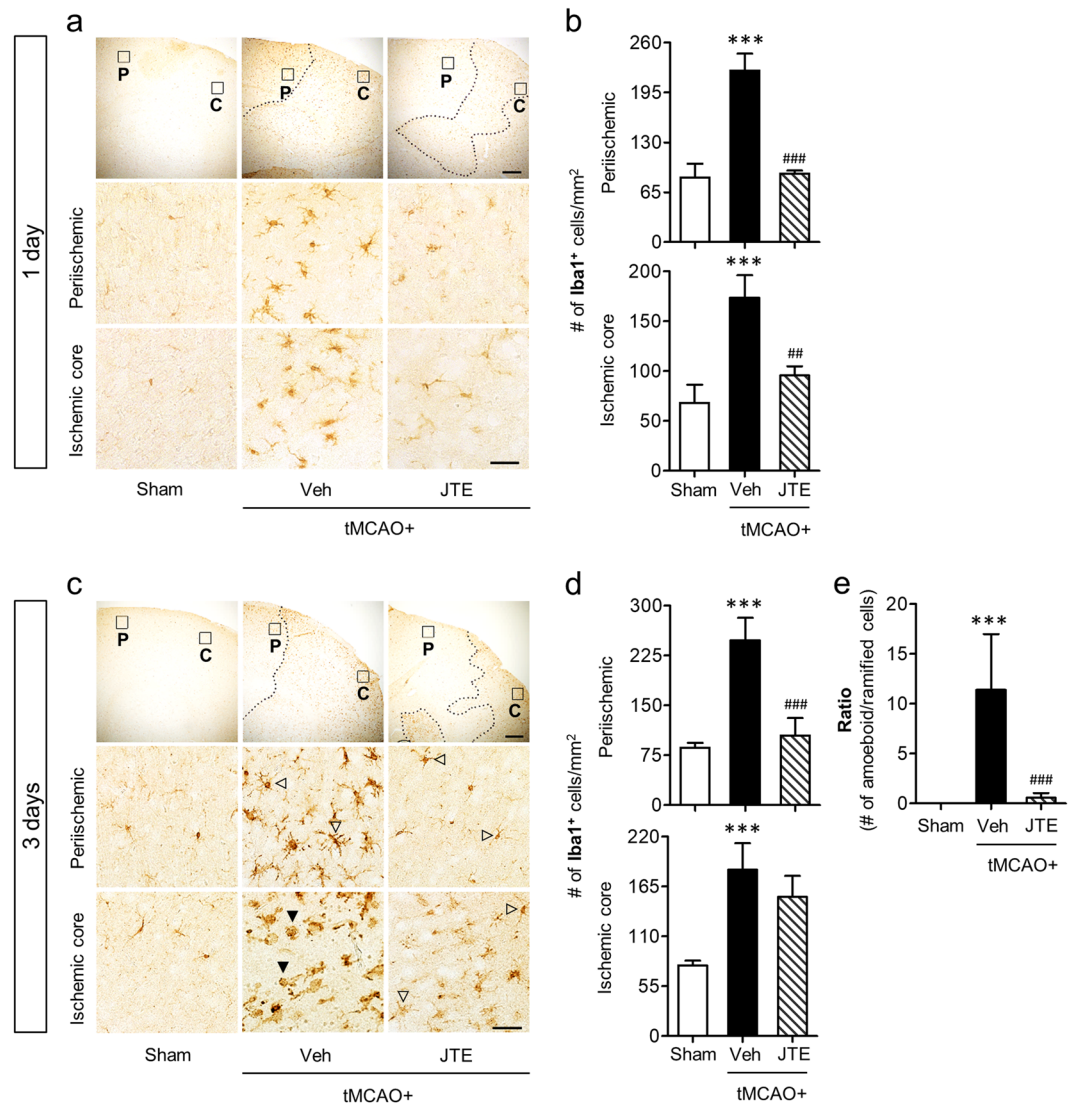


**Figure 1.** Suppressing S1P<sub>2</sub> activity reduces the number of Iba1-immunopositive cells in post-ischemic brain at 1 day and 3 days after tMCAO challenge. Effects of JTE013 (JTE) on microglia activation were observed by Iba1 immunohistochemical staining at 1 day (a,b) and 3 days (c–e). (a,c) Representative photographs of Iba1-immunopositive cells in periischemic (P) and ischemic core (C) regions at 1 day (a) and 3 days (c). Diagram box in the upper panel shows the cerebral area where images in middle and bottom panels are obtained. Dotted lines separate periischemic and ischemic core regions. Open arrowheads indicate ramified microglia and closed arrowheads indicate amoeboid microglia (c). Scale bars, 200  $\mu$ m (top) and 50  $\mu$ m (middle and bottom). (b,d,e) Quantification of Iba1 immunopositive cells in cells per mm<sup>2</sup> in both regions (b,d) and the ratio of amoeboid to ramified microglia (e). n = 4–5 mice per group. \*\*\**p* < 0.001 vs. sham; \*\**p* < 0.01 and ###*p* < 0.001 vs. vehicle-treated group by Newman-Keuls multiple range test.

3 days (Fig. 3). Such enhanced M1 polarization in post-ischemic brain was significantly attenuated by suppressing S1P<sub>2</sub> activity with JTE013 administration (Fig. 3). These data clearly demonstrate that S1P<sub>2</sub> signaling directs pro-inflammatory M1 polarization in post-ischemic brain. However, suppressing S1P<sub>2</sub> activity did not enhance anti-inflammatory M2 phenotypes, which was determined by measuring mRNA expression levels of M2 markers (CD206, IL-10, Arg-1, TGF- $\beta$ 1, YM1, and CCL-22) (Fig. 4). In some cases, it rather reduced mRNA expression levels of M2 markers (YM1 and CCL-22 in 1-day post-ischemic brain and Arg-1 and YM1 in 3-day post-ischemic brain). Altogether, these results demonstrate that S1P<sub>2</sub> signaling skews microglia towards mostly M1 polarization in injured brain after ischemic challenge.

In cerebral ischemia, M1 polarization mainly occurs in activated microglia<sup>11,30</sup>. Therefore, we next investigated whether the currently revealed S1P<sub>2</sub>-driven M1 polarization in post-ischemic brain occurred in activated microglia by determining a critical factor for M1 polarization, NF- $\kappa$ B activation, in activated microglia<sup>11,31</sup>. For this, we employed NF- $\kappa$ B(p65)/Iba1 double-immunofluorescence staining. As expected, NF- $\kappa$ B was activated in the brain both at 1 day (Fig. 5a,b) and 3 days (Fig. 5c,d) after tMCAO challenge. Most NF- $\kappa$ B(p65) signals were observed in Iba1-immunopositive cells (Fig. 5), strongly demonstrating that activated microglia were the loci for

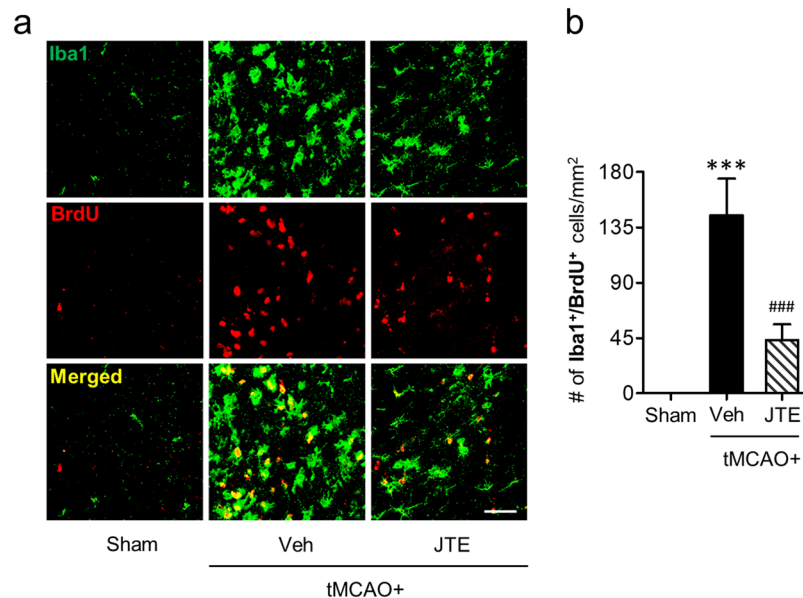


**Figure 2.** Suppressing S1P<sub>2</sub> activity attenuates microglial proliferation in post-ischemic brain. Brain samples from sham, tMCAO, and tMCAO mice exposed to JTE013 (JTE) were used to determine the proliferation of microglial cell through Iba1 and BrdU double immunohistochemical labelling at 3 days after tMCAO challenge. (a) Representative photographs of Iba1 and BrdU immunopositive cells in penumbra regions (region between periischemic and ischemic areas). Scale bar, 50  $\mu$ m. (b) Quantification of the number of Iba1 and BrdU double immunopositive cells in cells per mm<sup>2</sup>. n = 5 mice per group. \*\*\**p* < 0.001 vs. sham; ###*p* < 0.001 vs. vehicle-treated group by Newman-Keuls multiple range test.

M1 polarization in post-ischemic brain. This NF- $\kappa$ B activation in activated microglia was significantly attenuated by JTE013 administration (Fig. 5), further demonstrating that S1P<sub>2</sub> could regulate M1 microglial polarization in post-ischemic brain.

The current *in vivo* study demonstrated that S1P<sub>2</sub> could direct M1 polarization in cerebral ischemia. To reaffirm this notion *in vitro*, we used BV2 microglia cell line and treated cells with LPS, a well-known inducer of M1 polarization<sup>5,37</sup>. Upon LPS stimulation, mRNA levels of M1 soluble markers such as TNF- $\alpha$ , IL-1 $\beta$ , and IL-6 were upregulated in BV2 microglia (Fig. 6a–c). However, they were markedly attenuated by JTE013 exposure (Fig. 6a–c). Similarly, S1P<sub>2</sub> knockdown (Fig. 6d) attenuated mRNA expression levels of M1 soluble markers, except IL-1 $\beta$  (Fig. 6e–g). These *in vitro* data clearly demonstrate that S1P<sub>2</sub> is a critical factor for skewing microglia into M1 phenotypes, further supporting that S1P<sub>2</sub> could contribute to ischemic brain injury by directing microglial M1 polarization.

**Suppressing S1P<sub>2</sub> activity attenuates M1-relevant ERK1/2 and JNK MAPKs phosphorylation in post-ischemic brain and LPS-stimulated BV2 microglia.** The current *in vivo* and *in vitro* findings demonstrated that S1P<sub>2</sub> could drive M1 polarization in post-ischemic brain. Among S1P<sub>2</sub>-triggered effector pathways, G<sub>i</sub>-mediated MAPKs signaling pathways are well known effector pathways for M1 polarization<sup>38–40</sup>. Therefore, we sought to determine whether MAPKs might be involved in S1P<sub>2</sub>-driven M1 polarization. When BV2 microglia were polarized into M1 phenotype with LPS exposure, all three MAPKs (ERK1/2, p38 MAPK, and JNK MAPK) were activated as evidenced by their increased phosphorylation (Fig. 7a,b). Interestingly, ERK1/2 and JNK MAPK, but not p38 MAPK, were influenced by S1P<sub>2</sub>. Suppressing S1P<sub>2</sub> activity by JTE013 exposure significantly attenuated the phosphorylation of ERK1/2 and JNK (Fig. 7a,b), which was reaffirmed upon S1P<sub>2</sub> knockdown (Fig. 7c,d). These *in vitro* data demonstrated that S1P<sub>2</sub> enhanced phenotypical changes of microglia into M1 polarization through activating its effector pathways, ERK1/2 and JNK. We further determined whether these effector pathways were regulated by S1P<sub>2</sub> in post-ischemic brain. In the vehicle-treated group, phosphorylation levels of all three MAPKs (ERK1/2, p38, and JNK) were significantly increased in post-ischemic brain (Fig. 8a,b). Suppressing S1P<sub>2</sub> activity by JTE013 administration significantly attenuated the phosphorylation of ERK1/2 and JNK, but not that of p38 (Fig. 8a,b). These *in vivo* data demonstrated that S1P<sub>2</sub> influenced M1 polarization through ERK1/2 and JNK pathways in post-ischemic brain.

## Discussion

S1P receptors have been revealed as valuable therapeutic targets to treat cerebral ischemia due to successful results in validating FTY720's efficacy in human patients and animal models. Along with this success, some S1P receptor subtypes that can mediate pathogenesis of cerebral ischemia have been identified, including S1P<sub>1</sub><sup>24</sup> and S1P<sub>3</sub><sup>11</sup>, both of which are target receptor subtypes of FTY720<sup>41</sup>. In addition to FTY720-relevant receptor subtypes, S1P<sub>2</sub> that is not a target receptor subtype of FTY720 has been revealed as a pathogenic factor for cerebral ischemia<sup>25</sup>. Thus, up to now, three different S1P receptor subtypes have been identified to contribute to brain



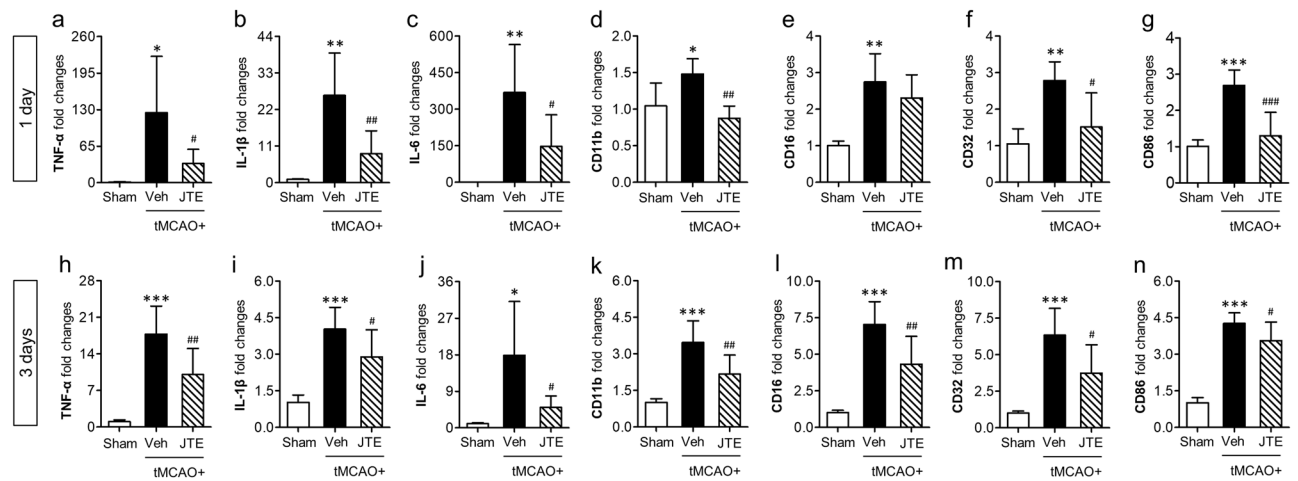


**Figure 3.** Suppressing S1P<sub>2</sub> activity downregulates mRNA expression levels of markers for M1 polarization in post-ischemic brain. Ipsilateral brain hemispheres from sham, tMCAO, and tMCAO mice exposed to JTE013 (JTE) were used to analyze changes in expression level of M1 markers including TNF- $\alpha$ , IL-1 $\beta$ , IL-6, CD11b, CD16, CD32, and CD86 by qRT-PCR analysis at 1 day (a–g) and 3 days (h–n) after tMCAO challenge.  $n = 5–6$  mice per group. \* $p < 0.05$ , \*\* $p < 0.01$ , and \*\*\* $p < 0.001$  vs. sham; # $p < 0.05$ , ## $p < 0.01$ , and ### $p < 0.001$  vs. vehicle-treated group by Newman-Keuls multiple range test.

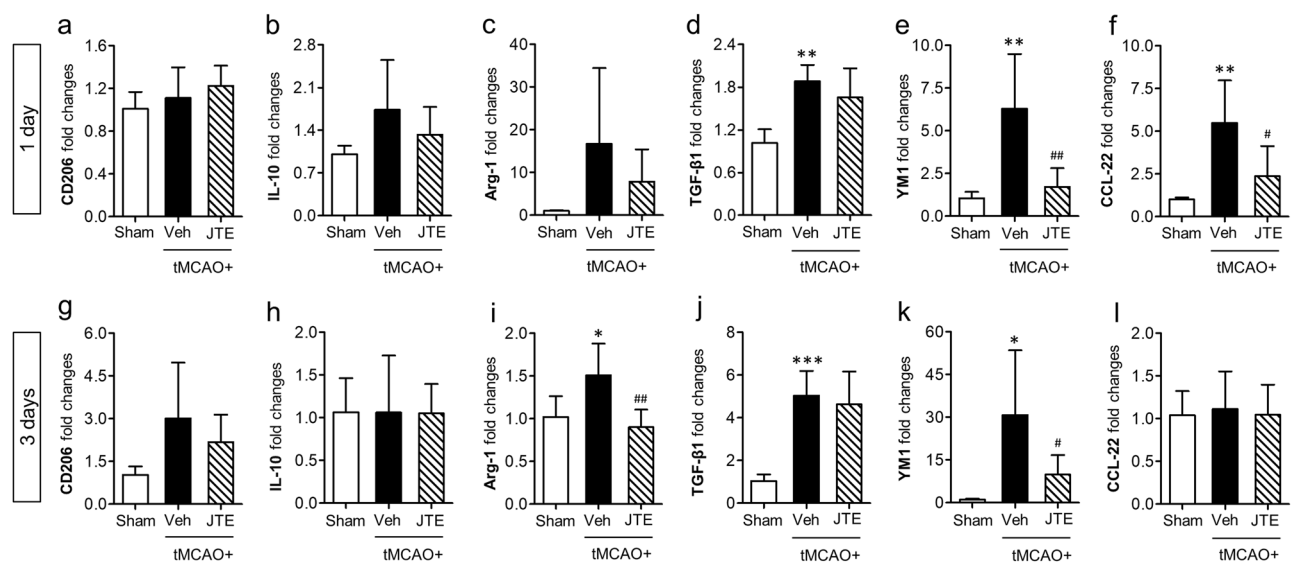


**Figure 4.** Suppressing S1P<sub>2</sub> activity does not enhance mRNA expression levels of markers for M2 polarization in post-ischemic brain. Ipsilateral brain hemispheres from sham, tMCAO, and tMCAO mice exposed to JTE013 (JTE) were used to analyze changes in expression level of M2 markers, including CD206, IL-10, Arg-1, TGF- $\beta$ 1, YM1, and CCL-22 by using qRT-PCR analysis at 1 day (a–f) and 3 days (g–l) after tMCAO challenge.  $n = 5–6$  per group. \* $p < 0.05$ , \*\* $p < 0.01$ , and \*\*\* $p < 0.001$  vs. sham; # $p < 0.05$  and ## $p < 0.01$  vs. vehicle-treated group by Newman-Keuls multiple range test.

injury in cerebral ischemia. In view of pathogenic mechanisms, it has been reported that these receptors can mediate different pathogenesis. S1P<sub>1</sub> and S1P<sub>3</sub> regulate microglial activation to act their detrimental roles in an ischemic brain<sup>11,24</sup> while S1P<sub>2</sub> mediates cerebrovascular dysfunction<sup>25</sup>. However, the identified pathogenesis might be part of diverse mechanisms. In fact, S1P<sub>1</sub> is also involved in cerebrovascular dysfunction after ischemic challenge<sup>24</sup>. S1P<sub>3</sub> is also associated with impaired vascular permeability in brain tumor<sup>42</sup>. Therefore, there might be more diverse mechanisms associated with each S1P receptor-dependent brain injury in cerebral ischemia. In this context, S1P<sub>2</sub> could trigger another pathogenic event in post-ischemic brain in addition to cerebrovascular dysfunction. This was addressed in the present study. The current study revealed that S1P<sub>2</sub> in post-ischemic brain was closely associated with microglial activation, a core pathogenesis in cerebral ischemia. Suppressing S1P<sub>2</sub> activity by JTE013 administration attenuated microglial activation, proliferation, morphological changes into

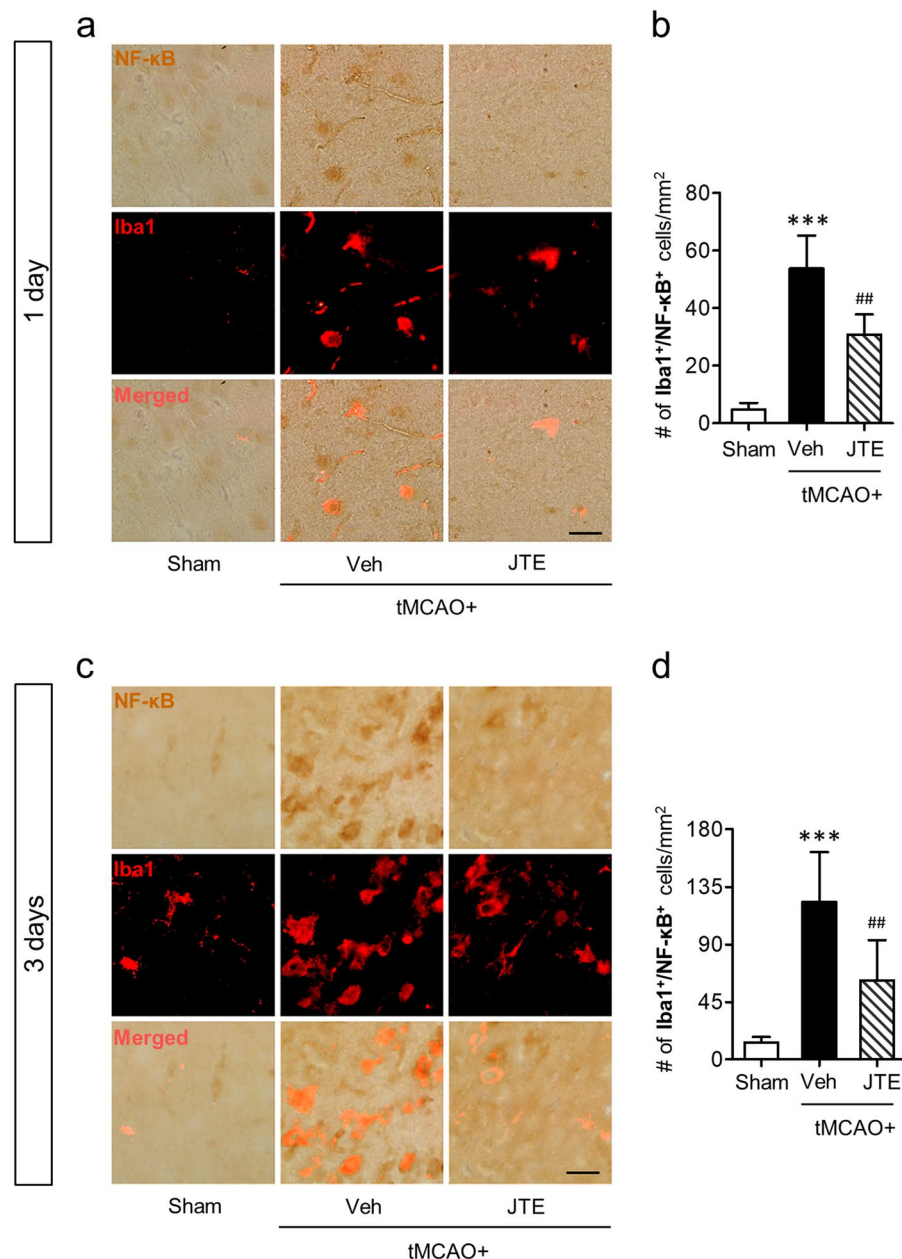


**Figure 5.** Suppressing S1P<sub>2</sub> activity attenuates microglial NF-κB activation in post-ischemic brain. Effects of JTE013 (JTE) on NF-κB expression in activation microglia were observed by Iba1/NF-κB double immunohistochemistry. **(a,c)** Representative photographs of Iba1/NF-κB double immunopositive cells in the post-ischemic brain at 1 day **(a)** and 3 days **(c)** after tMCAO challenge. **(b,d)** Quantification of the number of Iba1/NF-κB double immunopositive cells in cells per mm<sup>2</sup> at 1 day **(b)** and 3 days **(d)** after tMCAO challenge. n = 4–5 mice per group. Scale bar, 50 μm. \*\*\**p* < 0.001 vs. sham; ##*p* < 0.01 vs. vehicle-treated group by Newman-Keuls multiple range test.

toxic amoeboid shape, and M1 polarization, all of which indicated that S1P<sub>2</sub> could drive microglia toward detrimental functions, leading to brain damage.

Receptor-mediated S1P<sub>2</sub> signaling is well characterized in inflammatory diseases, both in peripheral tissues and CNS<sup>25–28,43</sup>. S1P<sub>2</sub> aggravates disease pathogenesis of bleomycin-induced pulmonary fibrosis by producing proinflammatory mediators, including TNF-α, IL-1β, IL-6, and monocyte chemoattractant protein (MCP)<sup>26</sup>. Similar proinflammatory roles of S1P<sub>2</sub> have been reported in renal ischemic injury, in which S1P<sub>2</sub> antagonism with JTE013 administration can protect renal cells by downregulating mRNA expression of proinflammatory mediators such as TNF-α, ICAM-1, MCP-1, and MIP-2<sup>27</sup>. S1P<sub>2</sub> is also associated with vascular inflammation as it increases vascular permeability through endothelial NF-κB activation<sup>28</sup>. These independent studies emphasizing proinflammatory roles of S1P<sub>2</sub> in peripheral tissues indicate that S1P<sub>2</sub> could modulate inflammatory cascades in post-ischemic brain as well. Indeed, recent reports have suggested that S1P<sub>2</sub> plays critical roles in aggravating

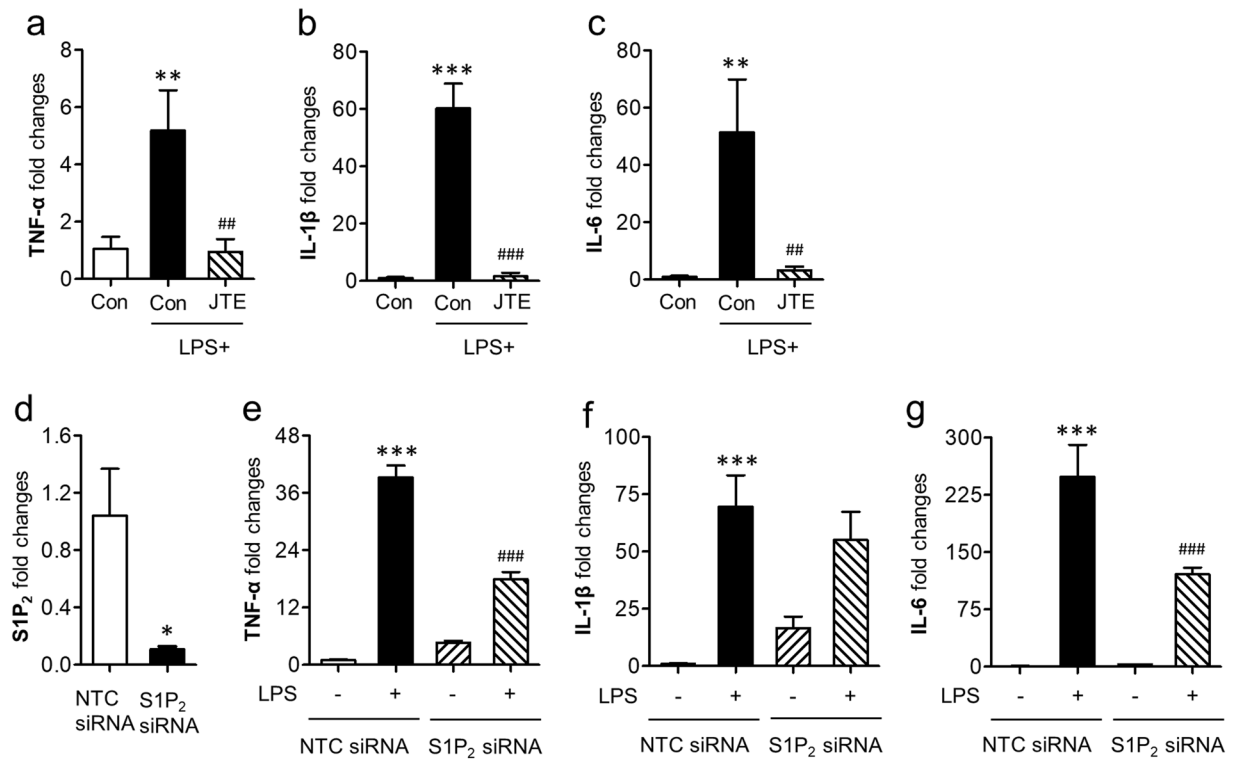


**Figure 6.** Suppressing S1P<sub>2</sub> activity downregulates mRNA expression levels of soluble markers for M1 polarization in LPS-stimulated BV2 microglia. Effects of JTE013 (JTE) (a–c) on LPS (100 ng/ml)-stimulated BV2 cells were determined by analyzing changes in expression level of M1 markers including TNF-α (a), IL-1β (b), and IL-6 (c) by qRT-PCR analysis. n = 3 per group. \*\**p* < 0.01 and \*\*\**p* < 0.001 vs. control (con); ##*p* < 0.01 and ###*p* < 0.001 vs. LPS-treated group by Newman-Keuls multiple range test. (d) Knockdown efficiency for S1P<sub>2</sub> was determined by qRT-PCR. n = 3 per group. \**p* < 0.05 vs. non-target control siRNA (NTC siRNA) by Mann-Whitney test. Effects of S1P<sub>2</sub> knockdown (e–g) on LPS (100 ng/ml)-stimulated BV2 cells were determined by analyzing changes in expression level of M1 markers including TNF-α (e), IL-1β (f), and IL-6 (g) by qRT-PCR analysis. n = 3 per group. \*\*\**p* < 0.001 vs. NTC siRNA; ###*p* < 0.001 vs. LPS-treated group infected with NTC siRNA (NTC siRNA + LPS) by Newman-Keuls multiple range test.

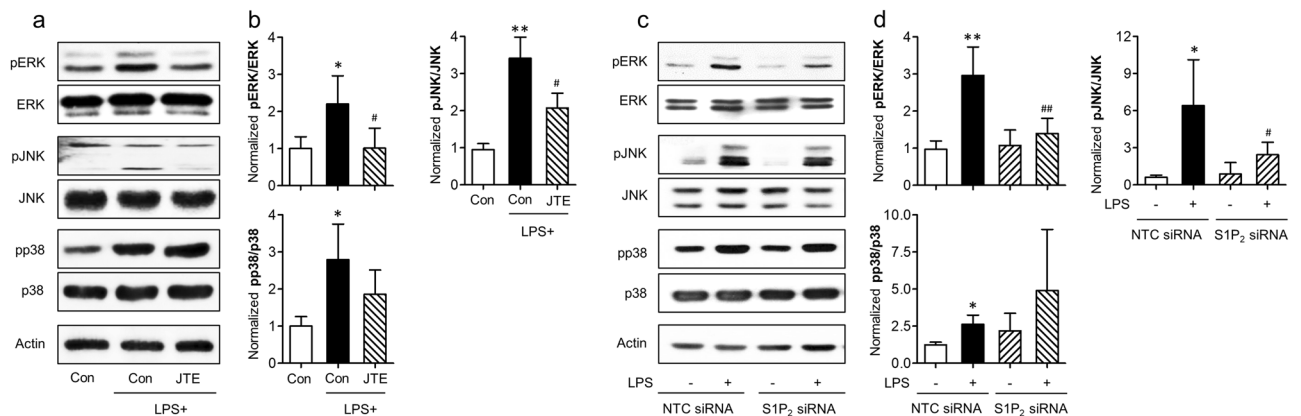


**Figure 7.** Suppressing S1P<sub>2</sub> activity attenuates phosphorylation of M1-relevant ERK1/2 and JNK MAPKs in LPS-stimulated BV2 microglia. Effects of JTE013 (JTE) (a,b) or S1P<sub>2</sub> knockdown (c,d) on LPS (1 μg/ml)-stimulated BV2 cells were determined by analyzing phosphorylation of ERK1/2, JNK, and p38 MAPKs through Western blot analysis. (a,c) Representative Western blots of each MAPK. (b,d) Quantification (n = 3 per group). \**p* < 0.05 and \*\**p* < 0.01 vs. control group (con, b) or control group transfected with non-target control siRNA (NTC siRNA, d); #*p* < 0.05 and ##*p* < 0.01 vs. LPS-treated group (b) or LPS-treated group transfected with NTC siRNA (NTC siRNA + LPS, d) by Newman-Keuls multiple range test.

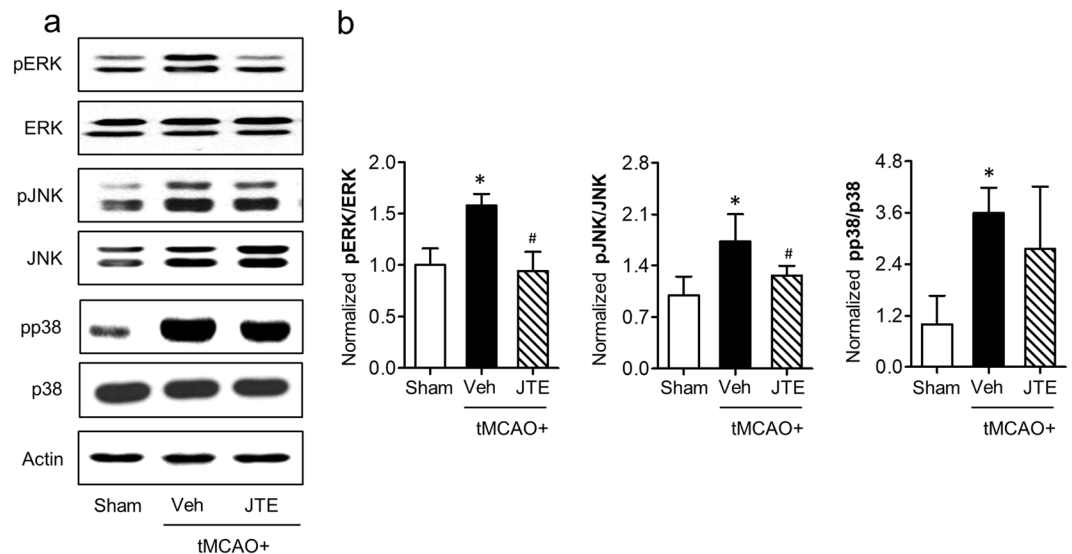


**Figure 8.** Suppressing S1P<sub>2</sub> activity attenuates phosphorylation of M1-relevant ERK1/2 and JNK MAPK in post-ischemic brain. Ipsilateral brain hemispheres from sham, tMCAO, and tMCAO mice exposed to JTE013 (JTE) were used to analyze phosphorylation of ERK1/2, JNK, and p38 MAPKs by Western blot analysis. **(a)** Representative Western blots of each MAPK. **(b)** Quantification (n = 4 mice per group). \**p* < 0.05 vs. sham; #*p* < 0.05 vs. vehicle-treated group by Newman-Keuls multiple range test.

neuroinflammation of post-ischemic brain through neurovascular inflammation<sup>25,43</sup>. Despite this clear link between S1P<sub>2</sub> and ischemia-induced neuroinflammation, whether S1P<sub>2</sub> regulates microglial activation, a key inflammatory event in post-ischemic brain, has not been revealed yet. The current study addressed this issue and provided a novel S1P<sub>2</sub>-mediated event, S1P<sub>2</sub>-regulated microglial activation in post-ischemic brain. Suppressing S1P<sub>2</sub> activity dramatically reduced the number of activated microglia, decreased proliferation of activated microglia, and reversed morphology of activated microglia from amoeboid cells into ramified cells in post-ischemic brain after tMCAO challenge. Therefore, based on previous and current findings, we can conclude that S1P<sub>2</sub> contributes to brain injury after ischemic challenge by aggravating immune responses in the brain through both vascular inflammation<sup>25,43</sup> and microglial activation (the current study). The latter was further supported by a recent study, demonstrating that suppressing S1P<sub>2</sub> activity by JTE013 exposure attenuated microglial activation and reduced proinflammatory responses in the cortex of mouse with hepatic encephalopathy<sup>33</sup>. Interestingly, these inflammatory roles have also been reported for S1P<sub>1</sub> and S1P<sub>3</sub>. S1P<sub>1</sub> and S1P<sub>3</sub> can trigger ischemic pathogenesis through microglial activation<sup>11,24</sup> and vascular inflammation<sup>24,42</sup> in post-ischemic brain, similar to S1P<sub>2</sub> (vascular inflammation<sup>25,43</sup> and microglial activation (current study)). In this notion, these three identified S1P receptor subtypes (S1P<sub>1</sub>, S1P<sub>2</sub>, and S1P<sub>3</sub>) as pathogenic factors for cerebral ischemia might share common pathogenesis for ischemic injury in the brain, likely neuroinflammation.

A critical feature of neuroinflammatory diseases including cerebral ischemia is that M1 and M2 polarization of immune cells can exert distinct responses: neurotoxic and neuroprotective. Particularly, increased number of amoeboid microglia is a strong indication for phenotypical changes into M1 polarization in injured brain because amoeboid microglia can act as detrimental cells to neurons following ischemic injury by secreting M1-relevant inflammatory mediators<sup>44,45</sup>. The current study revealed that S1P<sub>2</sub> was involved in triggering morphological transformation of microglia toward amoeboid shape, indicating that S1P<sub>2</sub> could mediate M1 microglial polarization. Indeed, we further demonstrated that S1P<sub>2</sub> triggered M1 polarization in post-ischemic brain as evidenced by attenuated mRNA upregulation of M1 surface and soluble markers upon suppressing S1P<sub>2</sub> activity. Importantly, activated microglia seem to be the main loci for this S1P<sub>2</sub>-regulated M1 polarization. NF- $\kappa$ B activation, a key mechanism for M1 polarization<sup>31,46</sup>, was observed mostly in activated microglia of post-ischemic brain. It was attenuated by suppressing S1P<sub>2</sub> activity in this study. This *in vivo* role of S1P<sub>2</sub> in M1 microglial polarization was further confirmed in BV2 murine microglia stimulated by using LPS, an inducer of M1 polarization. In these cells, suppressing S1P<sub>2</sub> activity significantly downregulated expression of functionally important M1 markers (TNF- $\alpha$ , IL-1 $\beta$ , and IL-6). Of note, S1P<sub>2</sub> seems to influence even more M1 polarization than M2 polarization in post-ischemic brain. In this study, suppressing S1P<sub>2</sub> activity did not show significant effects on M2 polarization in post-ischemic brain, although a few M2 markers were unexpectedly downregulated when S1P<sub>2</sub> activity was inhibited, indicating that S1P<sub>2</sub> could be mainly associated with promoting inflammatory M1 polarization rather than anti-inflammatory M2 polarization following ischemic injury. This notion can be further supported by a recent report suggesting the role of S1P<sub>2</sub> in macrophage polarization in peripheral tissues, in which suppressing S1P<sub>2</sub> activity attenuated M1 polarization of macrophages following liver injury<sup>47</sup>. Therefore, pathogenic roles of S1P<sub>2</sub> in post-ischemic brain can be mainly associated with suppression of inflammatory cascades through influencing M1 polarization rather than ischemic damage repair through M2 polarization.



Receptor-mediated S1P signaling exerts pleiotropic biological functions in different organs through intracellular effector pathways<sup>13</sup>. Among them, S1P receptors can commonly activate  $G_{\alpha i}$ -downstream signaling pathways that are mainly associated with M1/M2 polarization<sup>38–40,48</sup>. In particular,  $G_{\alpha i}$ -mediated activation of MAPKs is closely associated with M1 polarization through transcriptional activation of NF- $\kappa$ B<sup>38–40</sup>. Similarly, in this study, S1P<sub>2</sub>-regulated M1 polarization in activated microglia seemed to be mediated by activation of ERK1/2 and JNK MAPKs. Suppressing S1P<sub>2</sub> activity attenuated phosphorylation of ERK1/2 and JNK, but not that of p38 MAPK, in activated BV2 microglia towards M1 cells by LPS stimulation. Furthermore, in post-ischemic brain, activation of these two signaling molecules were dependent on S1P<sub>2</sub>. This might be the underlying mechanism for S1P<sub>2</sub> to regulate M1 polarization in post-ischemic brain.

Roles of S1P<sub>2</sub> in the current study was identified by the use of JTE013 because it has been known as an antagonist for S1P<sub>2</sub><sup>49,50</sup>. However, JTE013 could act on additional types of target. Its effects include agonist at S1P<sub>1</sub><sup>51</sup>, antagonist at S1P<sub>4</sub><sup>52</sup>, and blockers for other non-receptor targets<sup>53</sup>. Considering these previous reports, the currently observed effects of JTE013 could be mediated through its action at other targets. However, JTE013's effects might be irrelevant to S1P<sub>1</sub> activation because S1P<sub>1</sub> knockdown in the brain attenuated brain damage and microglial activation<sup>24</sup>. If JTE013 acted as an agonist for S1P<sub>1</sub>, it should potentiate brain damage and microglial activation. However, JTE013 administration reduced microglial activation (the current study) and brain damage following ischemic challenge (Kim *et al.*<sup>25</sup>; the current study). It might be also considerable that synthetic S1P<sub>1</sub> agonists such as FTY720 and AUY954 act as functional antagonists to S1P<sub>1</sub><sup>54,55</sup> and exert anti-inflammatory effects<sup>56,57</sup>. The observed effects of JTE013 in the current study might be mediated, in part, through S1P<sub>1</sub> if JTE013 acted as a functional antagonist to S1P<sub>1</sub>. Roles of S1P<sub>4</sub> in either cerebral ischemia or microglial activation remain unidentified, and therefore, it is unclear that JTE013 could exert its effects by acting on S1P<sub>4</sub>. JTE013 might also exert its effects by inhibiting KCl or endothelial thromboxane-1<sup>53</sup> because these two molecules were known to regulate ischemic brain damage<sup>58,59</sup>. Although we could not exclude possible involvement of other targets, it is clear that, at least, S1P<sub>2</sub> is involved in microglial activation and M1 polarization. In the current *in vitro* study, either JTE013 exposure or S1P<sub>2</sub> knockdown attenuated LPS-induced microglial M1 polarization and MAPKs phosphorylation. In addition, the current and previous *in vivo* studies have shown that either JTE013 treatment (the current study; Kim *et al.*<sup>25</sup>) or S1P<sub>2</sub> deletion in mice<sup>25</sup> reduces brain damage following ischemic challenge. These two independent studies support that JTE013's effects may be mediated through S1P<sub>2</sub> antagonism, further suggesting S1P<sub>2</sub> as a main player for microglial activation and M1 polarization after tMCAO challenge.

Iba1 has been widely used as a microglial marker for immunohistochemical analysis, but it can also be used as a marker for non-microglial cells, including monocyte/macrophages. In particular, robust infiltration of macrophages occurs in the ischemic core region at 3 days after tMCAO<sup>60,61</sup> because of blood brain barrier (BBB) disruption. Therefore, in the current study, Iba1-immunopositive cells in the ischemic core region at 3 days after tMCAO could be either activated microglia or infiltrated macrophages. However, many of the currently observed Iba1-immunopositive cells upon JTE013 administration could be more likely activated microglia. In fact, JTE013 administration after tMCAO remarkably attenuated BBB disruption<sup>25</sup>, suggesting that JTE013 administration could reduce macrophage infiltration into the ischemic core region. In contrast, JTE013 administration did not reduce total number of Iba1-immunopositive cells in the ischemic core region at 3 days after tMCAO, suggesting that most of the Iba1-immunopositive cells would be activated microglia rather than infiltrated macrophages.

In conclusion, we provided a new role of S1P<sub>2</sub> in ischemic pathogenesis such as microglial activation and M1 polarization, along with activation of its effector pathways including ERK1/2 and JNK. This study may provide a complementary pathogenic role of S1P<sub>2</sub> in cerebral ischemia in addition to previously provided roles of S1P<sub>2</sub> in neurovascular inflammation<sup>25,43</sup>. Up to now, three of five S1P receptor subtypes (S1P<sub>1</sub><sup>24</sup>, S1P<sub>2</sub> (the current study), and S1P<sub>3</sub><sup>11</sup>) have been identified as pathogenic factors for cerebral ischemia, all of which can influence microglial activation in post-ischemic brain. In particular, S1P<sub>2</sub> and S1P<sub>3</sub> could influence primarily M1 polarization in post-ischemic brain and activated microglia, whereas S1P<sub>1</sub> influenced both M1 and M2 polarization<sup>57</sup>. These S1P receptor subtypes can activate effector pathways in post-ischemic brain with a slightly different way. S1P<sub>1</sub> activates all 3 MAPKs (ERK1/2, p38, and JNK). S1P<sub>2</sub> activates ERK1/2 and JNK while S1P<sub>3</sub> activates ERK1/2 and p38 MAPK. Besides these three S1P receptor subtypes, it could not be excluded for remaining S1P receptor subtypes to be involved in ischemia-induced microglial activation and brain damage in cerebral ischemia.

## Methods

**Animals.** All animal experiments and handling were carried out under Center of Animal Care and Use (CACU) guidelines of Lee Gil Ya Cancer and Diabetes Institute (LCDI) at Gachon University, Korea (approved animal protocol number: LCDI-2017-0002). Male ICR mice (6 weeks old) were purchased from Orient Bio (GyeongGi-do, Korea).

**Transient focal cerebral ischemia challenge and drug administration.** Male ICR mice (7 weeks old) were used for transient middle cerebral artery occlusion (tMCAO) as previously described<sup>24</sup>. Briefly, mice were anesthetized with 3% isoflurane in 70% N<sub>2</sub>O:30% O<sub>2</sub> for induction and 1.5% for maintenance. Right middle cerebral artery (MCA) was occluded for 90 min by inserting a 9-mm-long 5-0 monofilament from the bifurcation of the common carotid artery to the MCA. Blood flow was restored by withdrawing the monofilament after 90 min. For the sham-operated group, the same surgical process was applied except for the occlusion. Mice that were subjected to tMCAO were randomly assigned into vehicle-treated and JTE013-treated groups. JTE013 (Cayman Chemical, MI, USA) was dissolved in 2% 2-hydroxypropyl  $\beta$ -cyclodextrin (Sigma-Aldrich, St. Louis, MO, USA) in saline and given orally to mice at 30 mg/kg immediately after reperfusion. The dose of JTE013 was chosen based on a previous study<sup>25</sup>. For the vehicle-treated group, equal volume of the vehicle was given. Four mice with hemorrhage were excluded for any data analysis throughout this study. In addition, three mice died within 24 h

following tMCAO challenge: one mouse was for a group of 1 day after tMCAO and two mice were for a group of 3 days after tMCAO.

**Neurological score analysis.** Functional neurological deficit was determined by modified neurological severity score (mNSS) 1 or 3 days after tMCAO. The mNSS was determined by motor, sensory, balance, and reflex tests with a total score ranging from 0 to 18 as described previously<sup>24,62</sup>.

**Tissue preparation for histological evaluation.** At 1 or 3 days after tMCAO, mice were anesthetized with a mixture of Zoletil 50<sup>®</sup> (Virbac Laboratories, Carros, France) and Rompun<sup>®</sup> (Bayer HealthCare LLC, Kansas 66201 U.S.A.) and perfused with ice-cold phosphate-buffered saline (PBS) followed by 4% paraformaldehyde (PFA) solution. Brains were removed, additionally fixed with 4% PFA, and cryoprotected with 30% sucrose solution. They were embedded in Tissue-Tek<sup>®</sup> optimal cutting temperature compound, frozen on dry ice, and cut into 20  $\mu$ m sections. To ensure anatomical similarities of brain regions in different experimental groups, two coronal brain sections obtained from the rostral to middle area of the striatum were used in histological experiments. For RNA and protein expression study, mice brains were transcardially washed with ice-cold PBS and ipsilateral brain hemispheres were harvested in liquid nitrogen.

**Fluoro-Jade B staining.** Neural cell death after tMCAO was determined by Fluoro-Jade B (FJB) staining. Sections were rinsed with water, incubated in alcohol series (100%, 70%, and 30%), and washed with water. They were oxidized with 0.06% potassium permanganate, rinsed with water, and stained with 0.001% FJB solution containing 0.1% acetic acid. These stained sections were washed with water, dried on a slide warmer, dehydrated with xylene, and mounted with Entellan medium.

**Iba1 immunohistochemistry staining.** To determine microglial activation at 1 or 3 days after tMCAO, brain sections were washed with PBS, treated with 1% H<sub>2</sub>O<sub>2</sub>, blocked with 1% fetal bovine serum (FBS) in 0.3% Triton X-100, and labeled with rabbit anti-Iba1 antibody (1:500, Wako Pure Chemicals, Osaka, Japan) overnight at 4 °C. Sections were incubated with a biotinylated secondary antibody (1:200, Santa Cruz, USA) and further incubated with avidin/biotin complex (ABC, 1:100, Vector Laboratories, Burlingame, CA, USA). To develop Iba1 signals, sections were treated with 0.02% 3,3'-diaminobenzidine tetrahydrochloride hydrate (DAB) (Sigma-Aldrich, St. Louis, MO, USA) solution containing 0.01% H<sub>2</sub>O<sub>2</sub>, rinsed with PBS, dehydrated in alcohol, cleared in xylene, and cover-slipped with Entellan medium.

**Bromodeoxyuridine (BrdU)/Iba1 double immunofluorescence staining.** Microglial proliferation in the brain after tMCAO challenge was determined by double immunofluorescence staining for BrdU and Iba1 at 3 days after tMCAO. BrdU (50 mg/kg, *i.p.*, Sigma-Aldrich St. Louis, MO, USA) was given twice a day at 12 h intervals for 2 days after tMCAO. Brain sections were fixed with 4% PFA, exposed to 2N HCl at 37 °C for DNA denaturation, and neutralized with borate buffer (0.1 M, pH 8.5). They were then blocked with 1% FBS in 0.3% Triton X-100 and labeled with primary antibodies against BrdU (1:200, Abcam, Cambridge, UK) and Iba1 (1:500) at 4 °C overnight. Sections were further labeled with secondary antibodies conjugated with Cy3 (1:1000, Jackson ImmunoResearch) and AF488 (1:1000, Invitrogen) and cover-slipped with VECTASHIELD<sup>®</sup> mounting media (Vector Laboratories, Burlingame, CA, USA).

**NF- $\kappa$ B/Iba1 double immunohistochemistry staining.** NF- $\kappa$ B signaling in activated microglia following tMCAO challenge was determined by NF- $\kappa$ B/Iba1 double immunohistochemistry staining as described previously<sup>11</sup>. Briefly, brain sections were fixed with 4% PFA, rinsed with PBS, and treated with Tris-EDTA solution at 100 °C for 30 min for antigen retrieval. Sections were blocked with 1% FBS in 0.3% Triton X-100 and incubated with rabbit NF- $\kappa$ B p65 (1:100, Santa Cruz, USA) antibody at 4 °C overnight. Sections were then incubated with biotinylated secondary antibody (1:200) at room temperature followed by incubating with ABC solution. Brain sections were then stained with DAB and washed with water. Stained sections with DAB were further labeled with a primary antibody against Iba1 (1:500) at 4 °C overnight. Sections were then incubated with a secondary antibody conjugated with Cy3 (1:1000) and mounted with VECTASHIELD<sup>®</sup> mounting media.

**Image preparation and quantification.** Brain images were obtained using a bright-field and fluorescence microscope equipped with a DP72 camera (BX53T, Olympus, Japan). Representative images were prepared using Adobe Photoshop Elements 8. For quantification, three images taken from different areas of each region were used for each mouse brain. The number of immunopositive cells were manually counted. The average number of cells is expressed in number of cells per unit area.

**Culture of BV2 microglia cell line and treatment.** Murine BV2 microglial cells were cultivated in Dulbecco's modified Eagle's medium (DMEM) supplemented with 10% FBS, penicillin, and streptomycin. Cells were seeded onto 6-well plates at a density  $2 \times 10^5$  cells/well. To induce M1 polarization, BV2 cells were exposed to LPS (*Escherichia coli* serotype 026:B6, Sigma-Aldrich, St. Louis, MO, USA) for 24 h. JTE013 (2  $\mu$ M) or vehicle (0.1% DMSO in DMEM) was added to cells at 30 min prior to LPS exposure. Alternatively, BV2 cells were transiently transfected with S1P<sub>2</sub> siRNA or non-target control siRNA (NTC siRNA) as described previously<sup>24</sup>. Forty-eight hours later, cells were exposed to LPS.

**Western blot.** Ipsilateral brain hemispheres were harvested at 24 h after tMCAO challenge and homogenized with neuronal protein extraction reagent. Protein samples from BV2 microglial cells were obtained at 1 h after LPS stimulation. Obtained proteins were separated through 10% SDS-PAGE, transferred to PVDF membrane, and blocked with 5% skim milk. These membranes were incubated with primary antibodies against rabbit

phosphorylated forms of MAPKs (pERK1/2, pp38, and pJNK; Cell Signaling, 1:1000), total forms of MAPKs (ERK1/2, p38, and JNK; Cell Signaling, 1:1000), and  $\beta$ -actin (Sigma Aldrich, 1:5000) at 4 °C overnight followed by incubation with respective secondary antibodies (Jackson ImmunoResearch, 1:10000) at room temperature for 2 h. Protein bands were visualized with enhanced chemiluminescence solution. Densitometric analysis was carried out using Image J software (National Institute of Mental Health, Bethesda, MD) and normalized with  $\beta$ -actin.

**Quantitative real-time PCR (qRT-PCR) analysis.** Total RNA was extracted from BV2 microglial cells or ipsilateral brain hemispheres using RNAiso plus (Takara, Kusatsu, Japan). For brain sampling, mice were perfused with autoclaved PBS and their brains were removed. Total RNA (1  $\mu$ g) was used to generate cDNA by reverse transcription using All-in-One First-Strand cDNA Synthesis SuperMix (TransGen Biotech, Haidian, China). Then mRNA expression levels of M1 and M2 polarization markers were determined using StepOnePlus™ qRT-PCR system (Applied Biosystems, Foster city, CA, USA) with FG Power SYBR Green PCR master mix (Life Technologies, Carlsbad, CA, USA) and specific primer sets (Supplementary Table 1). Expression levels of target genes were quantified using the  $2^{-\Delta\Delta CT}$  method relative to  $\beta$ -actin.

**Statistical analysis.** All data are presented as mean  $\pm$  standard deviation (SD). Statistical analysis was carried out using Mann-Whitney test for comparisons between two groups and one-way analysis of variance (ANOVA) followed by Newman-Keuls *post hoc* test for multiple comparisons using GraphPad Prism 5 (GraphPad Software Inc., La Jolla, CA, USA). Statistical significance was considered at  $p < 0.05$ .

### Data Availability

The data generated and analyzed as a part of this study are included within this article (as well as supplementary information).

### References

- Prinz, M. & Mildner, A. Microglia in the CNS: immigrants from another world. *Glia* **59**, 177–187, <https://doi.org/10.1002/glia.21104> (2011).
- Du, L. *et al.* Role of Microglia in Neurological Disorders and Their Potentials as a Therapeutic Target. *Mol Neurobiol* **54**, 7567–7584, <https://doi.org/10.1007/s12035-016-0245-0> (2017).
- Lin, L. L. & Little, J. W. Isolation and characterization of noncleavable (Ind-) mutants of the LexA repressor of Escherichia coli K-12. *J Bacteriol* **170**, 2163–2173 (1988).
- Qin, C. *et al.* Fingolimod Protects Against Ischemic White Matter Damage by Modulating Microglia Toward M2 Polarization via STAT3 Pathway. *Stroke* **48**, 3336–3346, <https://doi.org/10.1161/STROKEAHA.117.018505> (2017).
- Chhor, V. *et al.* Characterization of phenotype markers and neurotoxic potential of polarised primary microglia *in vitro*. *Brain Behav Immun* **32**, 70–85, <https://doi.org/10.1016/j.bbi.2013.02.005> (2013).
- Yenari, M. A., Kauppinen, T. M. & Swanson, R. A. Microglial activation in stroke: therapeutic targets. *Neurotherapeutics* **7**, 378–391, <https://doi.org/10.1016/j.nurt.2010.07.005> (2010).
- Zhao, S. C. *et al.* Regulation of microglial activation in stroke. *Acta Pharmacol Sin* **38**, 445–458, <https://doi.org/10.1038/aps.2016.162> (2017).
- Ito, D., Tanaka, K., Suzuki, S., Dembo, T. & Fukuuchi, Y. Enhanced expression of Iba1, ionized calcium-binding adapter molecule 1, after transient focal cerebral ischemia in rat brain. *Stroke* **32**, 1208–1215 (2001).
- Boscia, F. *et al.* NCX1 expression and functional activity increase in microglia invading the infarct core. *Stroke* **40**, 3608–3617, <https://doi.org/10.1161/STROKEAHA.109.557439> (2009).
- Gaire, B. P. *et al.* Neuroprotective effect of 6-paradol in focal cerebral ischemia involves the attenuation of neuroinflammatory responses in activated microglia. *PLoS One* **10**, e0120203, <https://doi.org/10.1371/journal.pone.0120203> (2015).
- Gaire, B. P., Song, M. R. & Choi, J. W. Sphingosine 1-phosphate receptor subtype 3 (S1P3) contributes to brain injury after transient focal cerebral ischemia via modulating microglial activation and their M1 polarization. *J Neuroinflammation* **15**, 284, <https://doi.org/10.1186/s12974-018-1323-1> (2018).
- Kanazawa, M., Ninomiya, I., Hatakeyama, M., Takahashi, T. & Shimohata, T. Microglia and Monocytes/Macrophages Polarization Reveal Novel Therapeutic Mechanism against Stroke. *Int J Mol Sci* **18**, <https://doi.org/10.3390/ijms18102135> (2017).
- Choi, J. W. & Chun, J. Lysophospholipids and their receptors in the central nervous system. *Biochim Biophys Acta* **1831**, 20–32, <https://doi.org/10.1016/j.bbalip.2012.07.015> (2013).
- Chun, J., Hla, T., Lynch, K. R., Spiegel, S. & Moolenaar, W. H. International Union of Basic and Clinical Pharmacology. LXXVIII. Lysophospholipid receptor nomenclature. *Pharmacol Rev* **62**, 579–587, <https://doi.org/10.1124/pr.110.003111> (2010).
- Fu, Y. *et al.* Fingolimod for the treatment of intracerebral hemorrhage: a 2-arm proof-of-concept study. *JAMA Neurol* **71**, 1092–1101, <https://doi.org/10.1001/jamaneurol.2014.1065> (2014).
- Fu, Y. *et al.* Impact of an immune modulator fingolimod on acute ischemic stroke. *Proc Natl Acad Sci USA* **111**, 18315–18320, <https://doi.org/10.1073/pnas.1416166111> (2014).
- Zhu, Z. *et al.* Combination of the Immune Modulator Fingolimod With Alteplase in Acute Ischemic Stroke: A Pilot Trial. *Circulation* **132**, 1104–1112, <https://doi.org/10.1161/CIRCULATIONAHA.115.016371> (2015).
- Czech, B. *et al.* The immunomodulatory sphingosine 1-phosphate analog FTY720 reduces lesion size and improves neurological outcome in a mouse model of cerebral ischemia. *Biochem Biophys Res Commun* **389**, 251–256, <https://doi.org/10.1016/j.bbrc.2009.08.142> (2009).
- Hasegawa, Y., Suzuki, H., Sozen, T., Rolland, W. & Zhang, J. H. Activation of sphingosine 1-phosphate receptor-1 by FTY720 is neuroprotective after ischemic stroke in rats. *Stroke* **41**, 368–374, <https://doi.org/10.1161/STROKEAHA.109.568899> (2010).
- Moon, E. *et al.* Exogenous S1P Exposure Potentiates Ischemic Stroke Damage That Is Reduced Possibly by Inhibiting S1P Receptor Signaling. *Mediators Inflamm* **2015**, 492659, <https://doi.org/10.1155/2015/492659> (2015).
- Nazari, M., Keshavarz, S., Rafati, A., Namavar, M. R. & Haghani, M. Fingolimod (FTY720) improves hippocampal synaptic plasticity and memory deficit in rats following focal cerebral ischemia. *Brain Res Bull* **124**, 95–102, <https://doi.org/10.1016/j.brainresbull.2016.04.004> (2016).
- Shichita, T. *et al.* Pivotal role of cerebral interleukin-17-producing gammadeltaT cells in the delayed phase of ischemic brain injury. *Nat Med* **15**, 946–950, <https://doi.org/10.1038/nm.1999> (2009).
- Wei, Y. *et al.* Fingolimod provides long-term protection in rodent models of cerebral ischemia. *Ann Neurol* **69**, 119–129, <https://doi.org/10.1002/ana.22186> (2011).
- Gaire, B. P. *et al.* Identification of Sphingosine 1-Phosphate Receptor Subtype 1 (S1P1) as a Pathogenic Factor in Transient Focal Cerebral Ischemia. *Mol Neurobiol* **55**, 2320–2332, <https://doi.org/10.1007/s12035-017-0468-8> (2018).

25. Kim, G. S. *et al.* Critical role of sphingosine-1-phosphate receptor-2 in the disruption of cerebrovascular integrity in experimental stroke. *Nat Commun* **6**, 7893, <https://doi.org/10.1038/ncomms8893> (2015).
26. Park, S. J. & Im, D. S. Deficiency of Sphingosine-1-Phosphate Receptor 2 (S1P2) Attenuates Bleomycin-Induced Pulmonary Fibrosis. *Biomol Ther (Seoul)*, <https://doi.org/10.4062/biomolther.2018.131> (2018).
27. Park, S. W., Kim, M., Brown, K. M., D'Agati, V. D. & Lee, H. T. Inhibition of sphingosine 1-phosphate receptor 2 protects against renal ischemia-reperfusion injury. *J Am Soc Nephrol* **23**, 266–280, <https://doi.org/10.1681/ASN.2011050503> (2012).
28. Zhang, G. *et al.* Critical role of sphingosine-1-phosphate receptor 2 (S1PR2) in acute vascular inflammation. *Blood* **122**, 443–455, <https://doi.org/10.1182/blood-2012-11-467191> (2013).
29. Skoura, A. *et al.* Sphingosine-1-phosphate receptor-2 function in myeloid cells regulates vascular inflammation and atherosclerosis. *Arterioscler Thromb Vasc Biol* **31**, 81–85, <https://doi.org/10.1161/ATVBAHA.110.213496> (2011).
30. Hu, X. *et al.* Microglia/macrophage polarization dynamics reveal novel mechanism of injury expansion after focal cerebral ischemia. *Stroke* **43**, 3063–3070, <https://doi.org/10.1161/STROKEAHA.112.659656> (2012).
31. Xia, C. Y., Zhang, S., Gao, Y., Wang, Z. Z. & Chen, N. H. Selective modulation of microglia polarization to M2 phenotype for stroke treatment. *Int Immunopharmacol* **25**, 377–382, <https://doi.org/10.1016/j.intimp.2015.02.019> (2015).
32. Foster, C. A. *et al.* Brain penetration of the oral immunomodulatory drug FTY720 and its phosphorylation in the central nervous system during experimental autoimmune encephalomyelitis: consequences for mode of action in multiple sclerosis. *J Pharmacol Exp Ther* **323**, 469–475, <https://doi.org/10.1124/jpet.107.127183> (2007).
33. McMillin, M. *et al.* Bile Acid-Mediated Sphingosine-1-Phosphate Receptor 2 Signaling Promotes Neuroinflammation during Hepatic Encephalopathy in Mice. *Front Cell Neurosci* **11**, 191, <https://doi.org/10.3389/fncel.2017.00191> (2017).
34. Ahmed, Z. *et al.* Actin-binding proteins coronin-1a and IBA-1 are effective microglial markers for immunohistochemistry. *J Histochem Cytochem* **55**, 687–700, <https://doi.org/10.1369/jhc.6A7156.2007> (2007).
35. Cherry, J. D., Olschowka, J. A. & O'Banion, M. K. Neuroinflammation and M2 microglia: the good, the bad, and the inflamed. *J Neuroinflammation* **11**, 98, <https://doi.org/10.1186/1742-2094-11-98> (2014).
36. Saijo, K. & Glass, C. K. Microglial cell origin and phenotypes in health and disease. *Nat Rev Immunol* **11**, 775–787, <https://doi.org/10.1038/nri3086> (2011).
37. Orihuela, R., McPherson, C. A. & Harry, G. J. Microglial M1/M2 polarization and metabolic states. *Br J Pharmacol* **173**, 649–665, <https://doi.org/10.1111/bph.13139> (2016).
38. Jiang, B., Brecher, P. & Cohen, R. A. Persistent activation of nuclear factor-kappaB by interleukin-1beta and subsequent inducible NO synthase expression requires extracellular signal-regulated kinase. *Arterioscler Thromb Vasc Biol* **21**, 1915–1920 (2001).
39. Olson, C. M. *et al.* p38 mitogen-activated protein kinase controls NF-kappaB transcriptional activation and tumor necrosis factor alpha production through RelA phosphorylation mediated by mitogen- and stress-activated protein kinase 1 in response to Borrelia burgdorferi antigens. *Infect Immun* **75**, 270–277, <https://doi.org/10.1128/IAI.01412-06> (2007).
40. Pan, Y. *et al.* Targeting JNK by a new curcumin analog to inhibit NF-kB-mediated expression of cell adhesion molecules attenuates renal macrophage infiltration and injury in diabetic mice. *PLoS one* **8**, e79084, <https://doi.org/10.1371/journal.pone.0079084> (2013).
41. Brinkmann, V. *et al.* The immune modulator FTY720 targets sphingosine 1-phosphate receptors. *J Biol Chem* **277**, 21453–21457, <https://doi.org/10.1074/jbc.C200176200> (2002).
42. Gril, B. *et al.* Reactive astrocytic S1P3 signaling modulates the blood-tumor barrier in brain metastases. *Nat Commun* **9**, 2705, <https://doi.org/10.1038/s41467-018-05030-w> (2018).
43. Wan, Y. *et al.* MicroRNA-149-5p regulates blood-brain barrier permeability after transient middle cerebral artery occlusion in rats by targeting S1PR2 of pericytes. *FASEB J* **32**, 3133–3148, <https://doi.org/10.1096/fj.201701121R> (2018).
44. Deng, Y., Lu, J., Sivakumar, V., Ling, E. A. & Kaur, C. Amoeboid microglia in the periventricular white matter induce oligodendrocyte damage through expression of proinflammatory cytokines via MAP kinase signaling pathway in hypoxic neonatal rats. *Brain Pathol* **18**, 387–400, <https://doi.org/10.1111/j.1750-3639.2008.00138.x> (2008).
45. Tam, W. Y. & Ma, C. H. Bipolar/rod-shaped microglia are proliferating microglia with distinct M1/M2 phenotypes. *Sci Rep* **4**, 7279, <https://doi.org/10.1038/srep07279> (2014).
46. Liu, C. P. *et al.* NF-kappaB pathways are involved in M1 polarization of RAW 264.7 macrophage by polyporus polysaccharide in the tumor microenvironment. *PLoS One* **12**, e0188317, <https://doi.org/10.1371/journal.pone.0188317> (2017).
47. Yang, J. *et al.* Sphingosine 1-Phosphate (S1P)/S1P Receptor2/3 Axis Promotes Inflammatory M1 Polarization of Bone Marrow-Derived Monocyte/Macrophage via G(alpha)i/o/PI3K/JNK Pathway. *Cell Physiol Biochem* **49**, 1677–1693, <https://doi.org/10.1159/000493611> (2018).
48. Vergadi, E., Ieronymaki, E., Lyroni, K., Vaporidi, K. & Tsatsanis, C. Akt Signaling Pathway in Macrophage Activation and M1/M2 Polarization. *J Immunol* **198**, 1006–1014, <https://doi.org/10.4049/jimmunol.1601515> (2017).
49. Sanchez, T. *et al.* Induction of vascular permeability by the sphingosine-1-phosphate receptor-2 (S1P2R) and its downstream effectors ROCK and PTEN. *Arterioscler Thromb Vasc Biol* **27**, 1312–1318, <https://doi.org/10.1161/ATVBAHA.107.143735> (2007).
50. Arikawa, K. *et al.* Ligand-dependent inhibition of B16 melanoma cell migration and invasion via endogenous S1P2 G protein-coupled receptor. Requirement of inhibition of cellular RAC activity. *J Biol Chem* **278**, 32841–32851, <https://doi.org/10.1074/jbc.M305024200> (2003).
51. Li, C. *et al.* Sphingosine 1-phosphate receptor 2 antagonist JTE-013 increases the excitability of sensory neurons independently of the receptor. *J Neurophysiol* **108**, 1473–1483, <https://doi.org/10.1152/jn.00825.2011> (2012).
52. Long, J. S. *et al.* Sphingosine 1-phosphate receptor 4 uses HER2 (ERBB2) to regulate extracellular signal regulated kinase-1/2 in MDA-MB-453 breast cancer cells. *J Biol Chem* **285**, 35957–35966, <https://doi.org/10.1074/jbc.M110.117945> (2010).
53. Salomone, S. *et al.* Analysis of sphingosine 1-phosphate receptors involved in constriction of isolated cerebral arteries with receptor null mice and pharmacological tools. *Br J Pharmacol* **153**, 140–147, <https://doi.org/10.1038/sj.bjp.0707581> (2008).
54. Choi, J. W. *et al.* FTY720 (fingolimod) efficacy in an animal model of multiple sclerosis requires astrocyte sphingosine 1-phosphate receptor 1 (S1P1) modulation. *Proc Natl Acad Sci USA* **108**, 751–756, <https://doi.org/10.1073/pnas.1014154108> (2011).
55. Shea, B. S. *et al.* Prolonged exposure to sphingosine 1-phosphate receptor-1 agonists exacerbates vascular leak, fibrosis, and mortality after lung injury. *Am J Respir Cell Mol Biol* **43**, 662–673, <https://doi.org/10.1165/rcmb.2009-0345OC> (2010).
56. Serdar, M. *et al.* Fingolimod protects against neonatal white matter damage and long-term cognitive deficits caused by hyperoxia. *Brain Behav Immun* **52**, 106–119, <https://doi.org/10.1016/j.bbi.2015.10.004> (2016).
57. Gaire, B. P., Bae, Y. J. & Choi, J. W. S1P1 Regulates M1/M2 Polarization toward Brain Injury after Transient Focal Cerebral Ischemia. *Biomol Ther (Seoul)*, <https://doi.org/10.4062/biomolther.2019.005> (2019).
58. Dojo Soeandy, C. *et al.* Endothelin-1-mediated cerebral ischemia in mice: early cellular events and the role of caspase-3. *Apoptosis* **24**, 578–595, <https://doi.org/10.1007/s10495-019-01541-z> (2019).
59. Li, N. *et al.* Elevated Serum Potassium Concentration Alleviates Cerebral Ischemia-Reperfusion Injury via Mitochondrial Preservation. *Cell Physiol Biochem* **48**, 1664–1674, <https://doi.org/10.1159/000492289> (2018).
60. Anttila, J. E., Whitaker, K. W., Wires, E. S., Harvey, B. K. & Airavaara, M. Role of microglia in ischemic focal stroke and recovery: focus on Toll-like receptors. *Prog Neuropsychopharmacol Biol Psychiatry* **79**, 3–14, <https://doi.org/10.1016/j.pnpbp.2016.07.003> (2017).
61. Wattanani, S. *et al.* Monocyte-Derived Macrophages Contribute to Spontaneous Long-Term Functional Recovery after Stroke in Mice. *J Neurosci* **36**, 4182–4195, <https://doi.org/10.1523/JNEUROSCI.4317-15.2016> (2016).
62. Sapkota, A. *et al.* Eupatilin exerts neuroprotective effects in mice with transient focal cerebral ischemia by reducing microglial activation. *PLoS One* **12**, e0171479, <https://doi.org/10.1371/journal.pone.0171479> (2017).



## Acknowledgements

We thank YJ Bae for assistance with qRT-PCR and Western blot analyses. This work was supported by grants [NRF-2017R1A2B4002818 and NRF-2014M3A9B6069339] from the National Research Foundation (NRF) to J.W.C.

## Author Contributions

A.S., B.P.G. and J.W.C. designed the research. A.S., B.P.G. and M.K. carried out *in vivo* and *in vitro* experiments. A.S., B.P.G., and J.W.C. analyzed the data and wrote the manuscript. All authors read and approved the final manuscript.

## Additional Information

**Supplementary information** accompanies this paper at <https://doi.org/10.1038/s41598-019-48609-z>.

**Competing Interests:** The authors declare no competing interests.

**Publisher's note:** Springer Nature remains neutral with regard to jurisdictional claims in published maps and institutional affiliations.



**Open Access** This article is licensed under a Creative Commons Attribution 4.0 International License, which permits use, sharing, adaptation, distribution and reproduction in any medium or format, as long as you give appropriate credit to the original author(s) and the source, provide a link to the Creative Commons license, and indicate if changes were made. The images or other third party material in this article are included in the article's Creative Commons license, unless indicated otherwise in a credit line to the material. If material is not included in the article's Creative Commons license and your intended use is not permitted by statutory regulation or exceeds the permitted use, you will need to obtain permission directly from the copyright holder. To view a copy of this license, visit <http://creativecommons.org/licenses/by/4.0/>.

© The Author(s) 2019